Journal of Materials Chemistry C

Accepted Manuscript

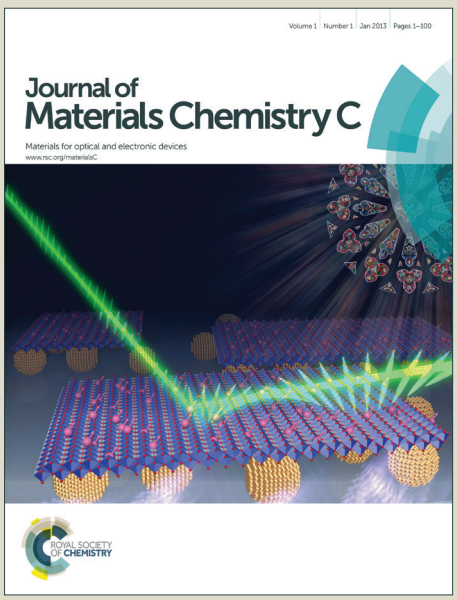

ROYAL SOCIETY OF CHEMISTRY

www.rsc.org/materialsC

Journal of Materials Chemistry C

PAPER

View Article Online
View Journal | View Issue

Cite this: DOI: 10.1039/xxxxxxxxxx

A Closer Look at the Light-Induced Changes in the Viscoelastic Properties of Azobenzene-Containing Polymers by Statistical Nanoindentation

Luca Sorelli,*[a] Filippo Fabbri,**[b] Jessy Frech-Baronet,[a] Anh-Duc Vu,[c] Mario Fafard,[a] Thierry Gacoin,[c] Khalid Lahlil,[c] Lucio Martinelli,[c] Yves Lassailly[c] and Jacques Peretti[c]

Received Date
Accepted Date

DOI: 10.1039/xxxxxxxxxx

www.rsc.org/journalname

The mechanical properties of azobenzene-containing polymer films are statistically measured by instrumented nanoindentation experiments in the dark and under illumination in the absorption band of the azobenzene molecules. The material is obtained from a commercial PMMA compound grafted with Dispersed Red 1 (DR1) azobenzene derivative. In the dark, DR1 molecules remain in the stable trans isomer state while, under illumination, they undergo photoisomerisation cycling and form a dynamic photo-stationary equilibrium between cis and trans isomers. This material is known to exhibit photomechanical properties related to the photoisomerization cycling of the DR1 units. Statistical loading/unloading tests performed in the tens of μN load range exhibit a significant change in the mechanical properties of the film under light excitation. The material's hardness and irreversible viscosity are all seen to decrease, while the creep coefficient value increases, revealing the occurrence of a viscoplastic behaviour of the film under illumination. Moreover, creep experiments performed at a constant load show a striking dissipative effect when light is turned on and also, surprisingly, when light is turned off. This behaviour is supposedly related to the rearrangement of the polymer chains when the balance between cis and trans isomer populations is modified either by illumination or by thermal activation when light is turned off.

1 Introduction

In recent years, materials incorporating azobenzene derivatives have drawn attention because of their singular mechanical response to a light stimulus.[1] The photo-mechanical properties of azo-materials stem from the isomerization of the azobenzene molecule between its trans (stable) and cis (meta-stable) configurations, subsequent to the absorption of a photon.[2] Since the first observation of the photoinduced deformation process in azopolymers[3,4] various photomechanical effects have been demonstrated over a wide scale range,[5,6] such as optical surface nanopatterning, membrane photoactuation, optical control of single objects and of fluid motion. These phenomena could potentially lead to new technological developments in various domains such as data storage, intelligent coatings, integrated optics, ophthalmic optics and display technologies. In this perspective, the development of processes involving azo-materials requires an in-depth understanding of the mechanisms at the origin of the photo-deformation, which is still not achieved, in spite of many experimental[7–12] and theoretical[13–24] efforts. In this context, relevant information could be obtained from the investigation of the photo-induced changes in the mechanical properties of the azo-materials, especially in thin films. Several studies are reported in the literature, but remain fragmentary and in some aspects contradictory. They are based on various experimental approaches and focused on different polymer materials incorporating different azobenzene derivatives. Two classes of azo-materials are commonly studied depending on the type of azo-derivatives: the azo-compounds with a long lifetime cis-isomer and the so-called donor-acceptor push-pull azobenzene derivatives, which exhibit fast cycling between the trans and cis configurations under illumination in their visible absorption band. The elastic compliance of thin polymer films containing an azobenzene derivative with a long cis lifetime has been measured by a quartz resonator tech-

[a] Département de Génie Civil, Université Laval, G1V 0A6 Québec, QC (Canada). Fax: 001 418 656-5343; Tel: 001 418 656-2131.
* E-mail: luca.sorelli@gci.ulaval.ca
[b] Institut d'Electronique Fondamentale, Université Paris-Sud/CNRS, 91405 Orsay (France).
** E-mail: filippo.fabbri@u-psud.fr
[c] Laboratoire de Physique de la Matière Condensée, Ecole Polytechnique/CNRS, 91128 Palaiseau (France).

nique.[25] A change in the high frequency compliance by a few percent is detected, which depends on the illumination wavelength: visible light irradiation leads to a slight increase in the elastic compliance, while UV illumination produces the opposite effect, that is a decrease in the compliance, although both illumination configurations are expected to favor the cis isomer population. These results are confirmed by electromechanical spectroscopy.[26] A possible explanation is that visible light causes a slight softening of the film, whereas UV light results in an initial plasticization of the material followed by its hardening. But the effect of UV illumination on the polymer itself is not considered.[27] Instrumented nanoindentation has also been used to characterize the photo-induced mechanical response of azo-PMMA polymer films in terms of elasticity in the static regime.[28] The results show a 10 % increase in the modulus upon UV irradiation while a partial recovery of the modulus is observed when illuminating with visible light. On the other hand, when films of azobenzene containing vinyl ethers in a polycarbonate matrix are subjected to tensile stress under UV and visible irradiation, a net decrease in the elastic modulus of 16 % and 10 %, respectively, is measured.[29]

Concerning experiments aimed at probing the mechanical properties of push-pull azobenzene containing films, interesting results were initially achieved by Atomic Force Microscopy nanoindentation at very low penetration depth (10-20 nm).[30] Upon illumination the elastic modulus is found to decrease by 74 % from 3.4 GPa to 0.9 GPa, as a consequence of the anisotropic fluidization along the direction parallel to the light polarization. The analysis of the creep response under constant load by fitting the Ting's formulation[31] of the Maxwell viscosity yields an estimated light induced viscosity of a 4.1 GPa s, which is three orders of magnitude less than the typical viscosity in the glassy state (10^3 GPa s).[32] From a mechanics point of view, the choice of the Maxwell model, which cannot describe the creep behavior of a viscoelastic polymer, may be questionable. Vapaavuori et al. have performed nanoindentation studies of azo-polymers with two types of chromophores exhibiting different bonding to the polymer backbone and different cycling rates under illumination in the visible absorption band.[33] In both cases, significant softening of the material is observed under visible illumination with a strong increase in the residual indentation depth that indicates the occurrence of a plastic deformation regime. More recently, for a similar material, Harrison et al. have evidenced a plastic photosoftening far beyond thermal effects together with a reduction of the Young's modulus by up to 50%.[34] However, a full picture in terms of viscoplasticity is not achieved, since the indentation dynamics is not analyzed. Let us finally mention the opposite behavior observed by Richter et al. who report a strong increase in the material stiffness and hardness upon illumination.[35] Moreover, the light-induced change in the mechanical property are mostly irreversible after switching off the light.

In the present work, we study the mechanical properties of PMMA thin films containing the Dispersed Red 1 (DR1) azobenzene derivative, which exhibits a strong push-pull character. We use a customized, highly accurate nanoindentation technique to perform a statistical characterization of the light-induced changes in the mechanical properties of material. The equipment provides an active reference which gives access to the dynamics and can be operated in the tens of μN load range which is mandatory to study thin films of soft materials. We confirm a slight decrease in the elastic modulus of the material upon illumination in the DR1 visible absorption band. Creep measurements are performed to characterize the dynamical response of the material. Hardness and creep coefficient exhibit significant changes with the illumination. Unloading tests allow us to determine separately the effect of light on both the reversible and irreversible contributions to the viscous deformation, showing a decrease in the irreversible viscosity by an order of magnitude. Finally, light switching under constant load evidences the role of the polymer chain reorganization related to the change in the DR1 isomers population balance.

2 Basics of nanoindentation

Nanoindentation has become a powerful technique to quantitatively measure the elasticity and hardness of soft polymer thin films.[36] During an indentation test schematized in **Figure 1a** the load P and the penetration depth h of the indenter into the material are simultaneously measured. A typical $P-h$ curve (**Figure 1b**) consists of a loading curve up to the maximum load P_{max} followed by an unloading curve. Note that the loading curve profile is always convex in the case of conical indenters, if there is no friction on the tip-material interface. Among the several existing types of indenter, we use the Berkovich-type indenter (**Figure 1a**), whose equivalent conical shape maximizes the tip sharpness and simple geometry is suitable for the interaction modelling. The Berkovich three-sided pyramidal diamond tip has an equivalent cone semi-angle $\theta = 70.3°$. The analysis of the $P-h$ curve hinges on applying a continuum model[37] to derive different indentation properties.

The indentation modulus M is directly related to geometrical parameters, A_c, the projected area of the indenter-sample contact and β the coefficient accounting for the slip on the indenter surface ($\beta = 1.034$ for the Berkovich-type indenter[37,38]):

$$M = \frac{S\sqrt{(\pi)}}{2\beta\sqrt{A_c}} \tag{1}$$

The indentation hardness H is equivalent to the mean pressure supported by the sample under maximum load:

$$H = \frac{P_{max}}{A_c} \tag{2}$$

The contact stiffness S is the slope measured during the initial stages of the unloading curve (**Figure 1b**):

$$S = \left(\frac{dP}{dh}\right)_{h=h_{max}} \tag{3}$$

The Young modulus E of an isotropic homogeneous material is estimated from the indentation modulus M as follows:

$$M^{-1} = \frac{1-\nu_i^2}{E_i} + \frac{1-\nu^2}{E} \tag{4}$$

where E_i and ν_i are the elastic modulus and Poisson's ratio of the diamond tip, equal to 1141 GPa and 0.07 respectively, while E and ν are the Young modulus and Poisson's ratio of the material.

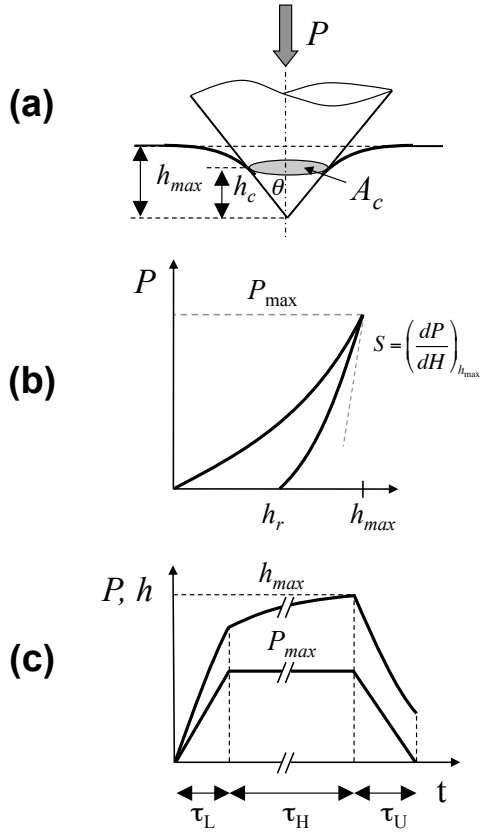

Fig. 1 (a) Schematic view of an indentation test with a conical indenter showing the relevant geometrical quantities: h_c the contact depth, h_{max} the maximum penetration depth and A_c and the projected contact area at maximum load. (b) Typical load vs. penetration depth $(P-h)$ curve, where h_r is the residual deformation after indentation and S the contact stiffness measured at peak load. (c) Load profile $P(t)$ and displacement $h(t)$ of the tip versus time during a creep experiment.

The material shear modulus G can be defined as $G=\frac{E}{2(1+\nu)}$. The projected contact area A_c depends on the contact depth h_c (**Figure 1a**). The $A_c(h_c)$ function of the diamond indenter is calibrated according to a standard procedure on a reference fused silica sample.[39] It is usually determined by the Oliver and Pharr method, which gives:

$$A_c = 3\sqrt{3}h_c^2 tan^2\theta \quad (5)$$

where $h_c = h_{max} - \varepsilon P_{max}/S$ with the geometric constant $\varepsilon = 0.72$ for a conical indenter.[39]

The viscoelasticity behaviour is determined by performing a creep experiment under a constant load. (**Figure 1c**) shows the typical variation of the load P and penetration depth h during this experiment. The load is progressively applied over a time τ_L. When the chosen maximum load P_{max} is reached, it is held constant over a time τ_H. Finally, the load is reduced to zero over a time τ_U. The indentation creep coefficient, C, is generally determined by:

$$C = [h(\tau_L+\tau_H) - h(\tau_L)]/h(\tau_L) \quad (6)$$

where $h(\tau_L+\tau_H)$ is the value of the penetration depth at the end of the holding phase and $h(\tau_L)$ is the value of the penetration depth at the end of the loading phase. It is assumed that both elastic and plastic deformation processes occur during the loading of the indenter and elastic deformations are retrieved during the unloading curve.

The creep curves are interpreted by the classical Burgers viscoplastic model, described by 4 parameters $(E_1, E_2, \eta_1, \eta_2)$, which corresponds to a combination of a Maxwell element with a spring and dashpot in series (E_1, η_1), which accounts for the irreversible creep, and a Kelvin-Voigt element with a spring and dashpot in parallel (E_2, η_2), which describes the reversible creep (**Figure 2**). This model is considered viscoplastic in the sense that it develops a plastic deformation by the snapshot η_1, which is visualised by the blue curve in **Figure 2**. The model has not a threshold in the sense that the plastic deformation occurs at any level of stress. When a load function as schematized in **Figure 2(c)** is applied, the variation of the penetration depth with time, for $\tau_L+\tau_H > t > \tau_L$, is:

$$h^2(t) = \frac{\pi}{2}\frac{P_{max}(1-\nu^2)}{tan\theta}\left[\frac{1}{E_1} + \frac{1}{E_2}\left(1-e^{\frac{-t}{\tau_2}}\right) + \frac{1}{\eta_1(1-\nu^2)}t\right] \quad (7)$$

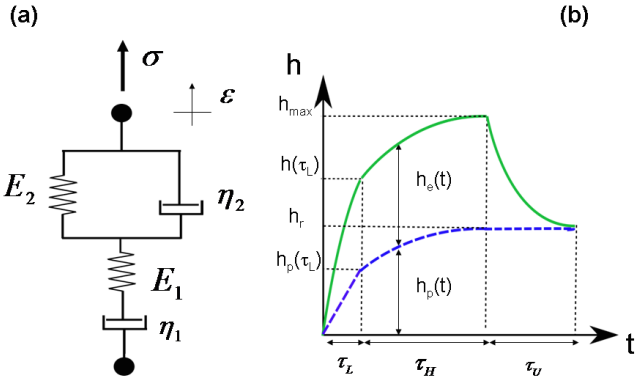

Fig. 2 (a). The material viscoplastic model considered in this study is the Burgers model which involves the viscosity coefficient η_i and the elastic modulus E_i of the material, where ε and σ are respectively the strain and applied stress.(b) Schematic $h-t$ curve showing the contribution of the elastic and irreversible deformations: h_r the residual deformation, h_{max} the maximum deformation, h_e the elastic deformation after loading and h_p the permanent deformation after loading. The blue curve represents the irreversible permanent $h_p(t)$ variation.

where $\tau_2 = \eta_2/E_2$ is the characteristic time of the reversible creep.[40] The irreversible permanent deformation $h_p(t)$ develops during the loading phase due to viscoplasticity as well as during the holding phase due to the Maxwell irreversible creep (**Figure 2b**). By assuming that the elastic modulus is constant during loading and unloading, the elastic penetration depth h_e for a conical indenter can easily be deduced from:[41]

$$h_e = \sqrt{\frac{\pi}{2}\frac{P_{max}(1-\nu^2)}{E_1 tan\theta}} \quad (8)$$

One can then simply estimate the permanent deformation depth $h_p = h - h_e$ during the holding phase and unloading phase,

with the hypothesis that unloading is purely elastic, as follows:

$$\tau_L + \tau_H > t > \tau_L : \quad (9)$$

$$h_p^2(t) = h_p^2(\tau_L) + \frac{\pi}{2}\frac{P_{max}\left(1-\nu^2\right)}{E_1 tan\theta}\frac{1}{\eta_1\left(1-\nu^2\right)}(t-\tau_L)$$

$$t > \tau_L + \tau_H : \quad (10)$$

$$h_p^2(t) = h_p^2(\tau_L) + \frac{\pi}{2}\frac{P_{max}\left(1-\nu^2\right)}{E_1 tan\theta}\frac{1}{\eta_1\left(1-\nu^2\right)}\tau_H$$

In this simplified model, we consider that the loading time τ_L and the unloading time τ_U are very short with respect to the holding time τ_H i.e. $\tau_L, \tau_U \ll \tau_H$. As a consequence, since the loading and unloading processes are very rapid, we assume that the entire creep occurs during the holding phase under constant load. From an energy point of view, the energy dissipated during an indentation test can be estimated as follows:

$$W_p = W_{tot} - W_{el} - W_{el}^{creep} = \int_0^{h(\tau_L)} P_{loading} dh \quad (11)$$

$$- \int_{h(\tau_L+\tau_U)}^{h(\tau_L+\tau_H+\tau_U)} P_{unloading} dh - \int_{h_p(\tau_L+\tau_U)}^{h(\tau_L+\tau_H+\tau_U)} P_{holding} dh$$

where W_{tot} is the total energy applied from the external force, W_{el} is the elastic energy recovered during the unloading and W_{el}^{creep} is the recoverable elastic energy due to the reversible part of creep. The latter term can be estimated as the elastic part of the applied load energy during the holding phase. Finally, the percentage of total energy dissipated is simply estimated by $\gamma_p = W_p/W_{tot}$.

3 Experiments

3.1 Sample preparation and characterization

The material studied here, thereafter referred as PMMA-DR1, is a PMMA organic polymer backbone with Disperse Red 1 (DR1) azobenzene derivative molecules grafted as side-chains. It is prepared from a solution of 25 mg of a commercial compound (Sigma-Aldrich 570435) in 100 *ml* of dichloromethane. The material absorption spectrum, shown in **Figure 3a**, exhibits a broad band centred at 487 nm, characteristic of the DR1 trans isomer, which is the stable chromophore conformation. Illumination in this absorption band generates a photo-stationary equilibrium between the DR1 trans and cis isomer populations: absorption of a photon induces a trans-to-cis conversion, while back-conversion to the trans configuration occurs either by thermal activation or by absorption of a photon (the DR1 cis isomer also exhibits an absorption band in the same visible range).[2]

The samples consist of 250-nm thick PMMA-DR1 films obtained by spin-coating the solution at 4000 rpm on a clean glass substrate. The photochrome concentration in the film is of about 1 molecule/nm^3. The photomechanical activity of the sample is checked by holographic inscription of a surface relief grating (SRG). An interference pattern produced by two linearly polarized beams, of wavelength 473 nm, in the absorption band of the azobenzene derivatives, is projected onto the sample through the glass substrate. The polarization of the beams are tilted by $\pm 45°$ with respect to the s polarization, which produces a polarization pattern of almost constant intensity. The density power and incidence angle of each beam are 1 mW cm^{-2} and 15.3°. The photoinduced change in the surface topography of the film is measured in real-time by coupled shear-force and scanning near field optical microscopy (**Figure 3b**). Before illumination, a surface roughness of about 0.5 nm RMS is observed, which is well below (at least by one order of magnitude) the values that could affect the nanoindentation measurements.[42,43] When the light is turned on, a surface relief grating forms, with a 900 nm period corresponding to the projected optical interference pattern. The photoinduced deformation amplitude kinetics during the first three minutes of illumination is shown in **Figure 3(c-d)**. It is comparable with previous results obtained on similar films of the same material.[44]

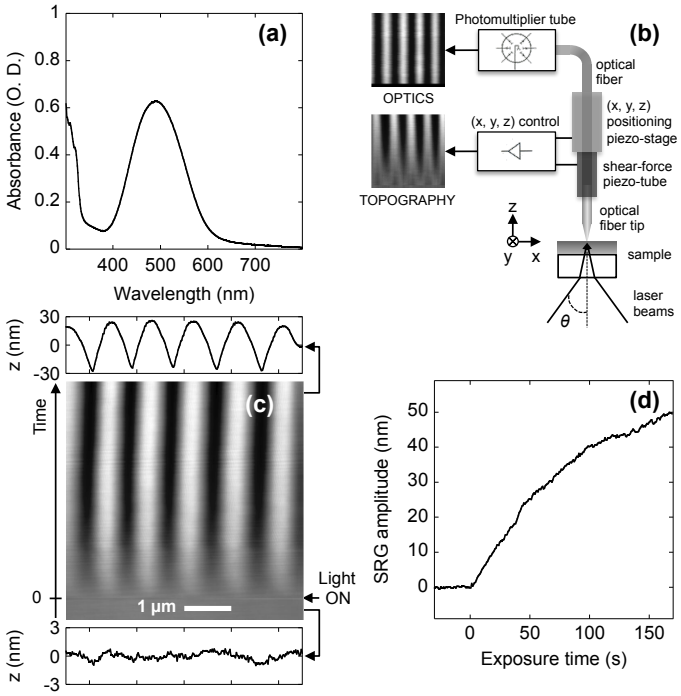

Fig. 3 (a) Absorption spectrum of the PMMA-DR1 molecule. (b) Schematics of the experimental setup enabling simultaneous recording of topographical and optical images. An interference pattern is projected on the sample through the glass substrate. (c) 5 μm $\times$ 5 μm shear-force image of the surface relief grating of 900 nm period recorded during the projection of the interference pattern on a 250 nm-thick azobenzene-containing PMMA thin film. The surface profile is measured before illumination, showing the surface roughness, and after 180 s of exposure, showing the SRG amplitude. (d) Variation of the surface relief amplitude as a function of the exposure time.

3.2 Experimental setup and procedure

The nanoindentation experimental setup is schematized in **Figure 4(a)**. We use a special Anton-Paar UNHT nanoindenter, endowed with an active reference system for differential measurement of

the indenter displacement, which allows reducing the thermal drift to less than 1 nm over 500 s.[45] This technique is especially suited for the study of very thin layers and soft materials and allows measuring time-dependent properties with great accuracy. Experiments are conducted on an anti-vibration stabilized table, in a room with controlled temperature ($20 \pm 1°$) and relative humidity ($30 \pm 2.5°$). The setup allows illumination of the sample through the glass substrate. A laser beam of wavelength $\lambda = 532$ nm, within the DR1 molecule absorption band, is used. The 2 mW laser beam illuminates an area of about 1 mm^2 around the nanoindenter tip apex location, with an incidence angle θ of about 30° in air. The laser is linearly polarized; its polarization direction is tilted by about 45° with respect to s-polarization.

A series of preliminary tests are carried out to determine the optimal penetration depth for the PMMA-DR1 thin film. The effect of the substrate can be often ignored by following a common rule of thumb that the maximum indentation depth should be limited to less than 10% of the film thickness.[39,46] In the case of the PMMA-DR1 films studied here, this corresponds to a maximum penetration depth $h_{max} \simeq 25$ nm. We found that the maximum load P_{max} required not to overcome this limit was of about 5 μN, a too low value to provide consistent reliable results. The penetration depth h_{max} was therefore increased step by step until the test repeatability was reliable, which was obtained for $P_{max} = 50$ μN and $h_{max} \simeq 80$ nm. As a consequence, since the ratio between the penetration depth (h_{max}) and the film thickness is 40% in our study, we performed experimental data analysis which takes into account the influence of the glass substrate.

Three experiments were then carried on which correspond to different combinations of loading profiles (LPs) with illumination profiles (IPs) as shown in **Figure 4(b)**. The LPs are characterized by three time constants: the loading time, τ_L, the holding time, τ_H, and the unloading time, τ_U.

In Experiment 1, the LP1 is applied to measure the viscoelastic properties of the sample in three distinct states: (i) the initial state, before any illumination (IP1); (ii) the excited state, during illumination with visible light (IP2); (iii) the relaxed state, 30 min after illumination is turned off (LP1). The loading is applied during the time $\tau_L = 8$ s. The load $P_{max} = 50$ μN is held during the time $\tau_H = 120$ s. The unloading occurs during the time $\tau_U = 8$ s until zero load is reached. The indentation measurements are repeated 25 times over a matrix of 5×5 indents with an inter-distance of 5 μm for each measurement.

In Experiment 2, LP2 is applied in order to perform creep recovery measurements in the dark (IP1) and during illumination (IP3). The load profile and holding phase are identical to Experiment 1. The unloading phase is performed in two steps: i) a partial unloading taking a time $\tau_U = 5$ s until $P_2 = 2.5$ μN; this load value is maintained during another holding phase of duration $\tau_H = 120$ s; ii) a final unloading phase to $P_2 = 0$, during a time $\tau_{U2} = 0.25$ s. Here again, the tests are repeated 25 times over a matrix of 5×5 indents with an inter-distance of 5 μm.

The Experiment 3 aims at studying the transitory behavior of the azo-material when the light is turned on and off during the indentation at constant load. LP1 is combined with IP4, with a holding time $\tau_H = 900$ s. The light is turned on 60 s after the beginning of the holding phase and is turned off 550 s later.

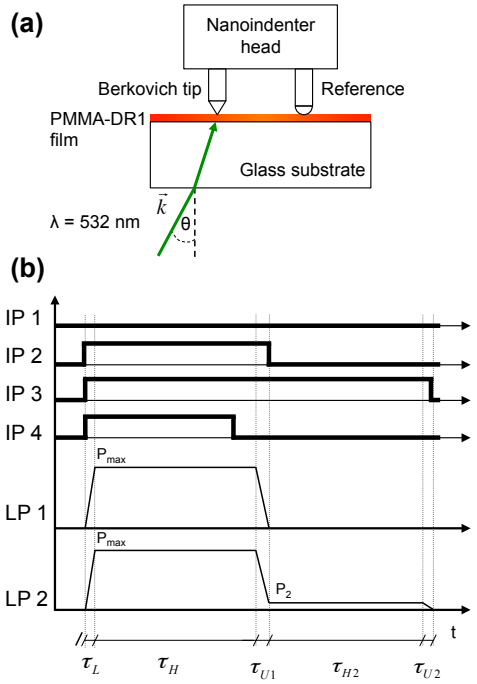

Fig. 4 (a) Schematics of the nanoindentation experimental setup with linearly polarized light excitation. Thanks to the active reference system, the indenter displacement is measured differentially with respect to the reference in contact with the sample surface. (b) Load profiles (LPs) and illumination profiles (IPs) applied in the various nanoindentation creep experiments.

4 Results

4.1 Nanoindentation tests on glass substrate

It is first mandatory to perform nanoindentation experiments on the bare glass substrate, in the dark and under illumination. As shown in **Figure 5**, the $P - h$ curves of a series of 50 tests are unaffected by the light. **Table 1** presents the mean values and standard deviations of the indentation Modulus (M), Hardness (H) and Creep coefficient (C) of the glass substrate deduced from these measurements, according to Equations (1), (2) and (6). Considering a Poisson's ratio of 0.22, the glass Young modulus is estimated to be 84.7 GPa. Such a value, slightly larger than the typical value for soda-lime float glass, was already reported.[47] This overestimation of the Young's modulus value derived from nanoindentation can be ascribed to an error in the determination of the contact area by the method of Oliver and Pharr, which neglects possible pile-up phenomena for penetration depth inferior to 150 nm.[48,49] The value of the glass substrate modulus derived from the measurements presented in **Figure 5**, leads to an overestimation of the stiffness of the film. In the present work, we did not attempt to correct this value but prefer to present a set of coherent raw data since we are mostly interested in evidencing and quantifying the change in the mechanical properties of the film under illumination rather than the precise absolute values of these properties.

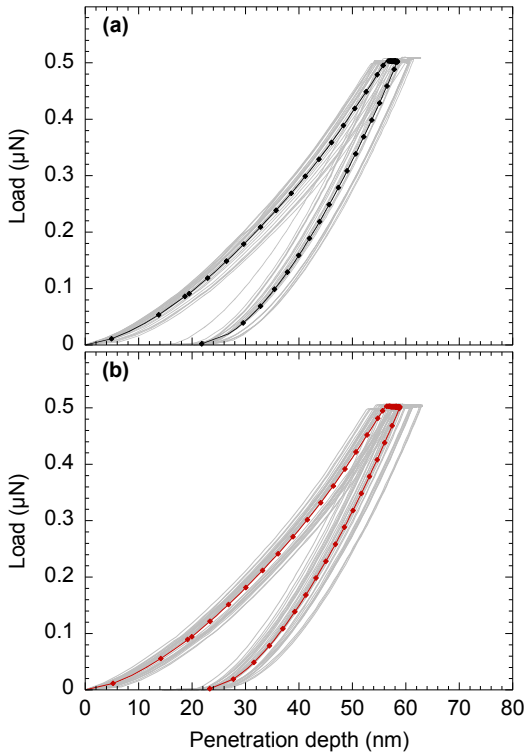

Fig. 5 $P-h$ curves for the glass substrate without (a) and with (b) optical excitation. Coloured symbols and curves correspond to the averages over 50 measurements.

4.2 Loading-unloading tests on PMMA-DR1 films

The statistical series of nanoindentation measurements following the procedure defined as Experiment 1, are presented in **Figure 6**. The initial state prior to illumination is characterized by the load-penetration ($P-h$) and penetration depth vs. time ($h-t$) curves shown in **Figure 6(a-b)**, respectively. The same measurements achieved during illumination and in the dark 30 minutes after illumination yield the curves (c-d) and the curves (e-f), respectively. The mean $P-h$ and $h-t$ curves (coloured curves and symbols) are compared for the 3 considered states in **Figure 6(g-h)**. The following conclusions can be drawn from the comparison between the three states. i) Illumination clearly increases the maximum penetration depth h_{max} by 30 %. ii) The relaxed state has the same quantitative mechanical response than the initial state, which asserts the reversible character of the mechanical changes induced by the photoisomerization of azobenzene molecules. iii) Unlike the initial state, the excited state reveals a large dispersion in the $P-h$ and $h-t$ curves which can hardly be attributed to the light intensity fluctuations.

Figure 7 compares the mean values of the indentation quantities (modulus M, hardness H, and creep coefficient C) for the initial excited and relaxed states. The value of the indentation modulus M, which reflects the stiffness of the material, is comparable to reported values for thick PMMA layers.[50] It slightly increases by about 8% when light is turned on and returns to the initial value when light is turned off. This result is in agreement with previous studies.[25,28,33] On the other hand, indentation hardness reduces by about 38% when light is turned on and gets back to its initial value when light is turned off. The most drastic variation concerns the indentation creep coefficient C, which increases by a factor of 2 under illumination. The standard deviation of the measured quantities remains quite low in the initial and relaxed states (4-5% for M and H, and 10% for C), but it significantly increases under illumination (7% for M and H, and 14% for C). This increase is related to the large dispersion observed in the $P-h$ and $h-t$ curves measured in the excited state.

Table 1 The indentation quantities estimated from the $P-h$ curves for the raw glass substrate with and without optical illumination. Standard deviation values deduced from the multiple tests are indicated.

Indentation quantity		Light OFF	Light ON
H [GPa]	Mean	9.06	9.28
	s.d.	0.81	0.82
M [GPa]	Mean	82.6	83.0
	s.d.	3.7	3.6
C [%]	Mean	4.65	3.61
	s.d.	1.49	2.50
γ_p [%]	Mean	0.39	0.38
	s.d.	0.04	0.06

All the indentation quantities M, H, and C retrieve their initial values when light is turned off, indicating that the photo-induced change in the mechanical properties of the film is almost completely reversible. Notably, the reduction in H and the increase in C suggest that the material exhibits a more pronounced viscoplastic behaviour under optical excitation, as will be confirmed later on by the creep-recovery experiments.

Several models have been developed to extract the intrinsic elastic modulus of thin films from the composite film/substrate modulus value obtained from indentation tests on coated systems. To estimate the modulus E_f of the azobenzene containing polymer film, we use a closed solution[51–54] for high contrast between the stiffness of the film and the substrate. In essence, the composite shear modulus G_c is:

$$\frac{1}{G_c} = (1-I_0)\frac{1}{G_s + F I_0 G_f} + I_0 \frac{1}{G_f} \tag{12}$$

which links the effective measured composite shear modulus G_c to the shear moduli of the film G_f and of the glass substrate G_s. According to the model proposed by Hay and Crawford,[51] the film gives two contributions to the overall shear modulus, which are weighted by two factors: the weight function I_0, which tends to weaken the contribution of the film when the penetration depth increases; and the parameter F, which is empirically introduced and estimated by finite element analysis to be 0.026. The expression of the weight function I_0 is:

$$\begin{aligned} I_0 &= \frac{2}{\pi}\arctan\left(\frac{d}{a}\right) \\ &+ \frac{1}{2\pi(1-\nu_c)}\frac{d}{a}\left\{(1-2\nu_c)\,ln\left[\frac{1+(d/a)^2}{(d/a)^2}\right] - \frac{1}{1+(d/a)^2}\right\} \end{aligned} \tag{13}$$

where d is the film thickness and a is the radius of the contact

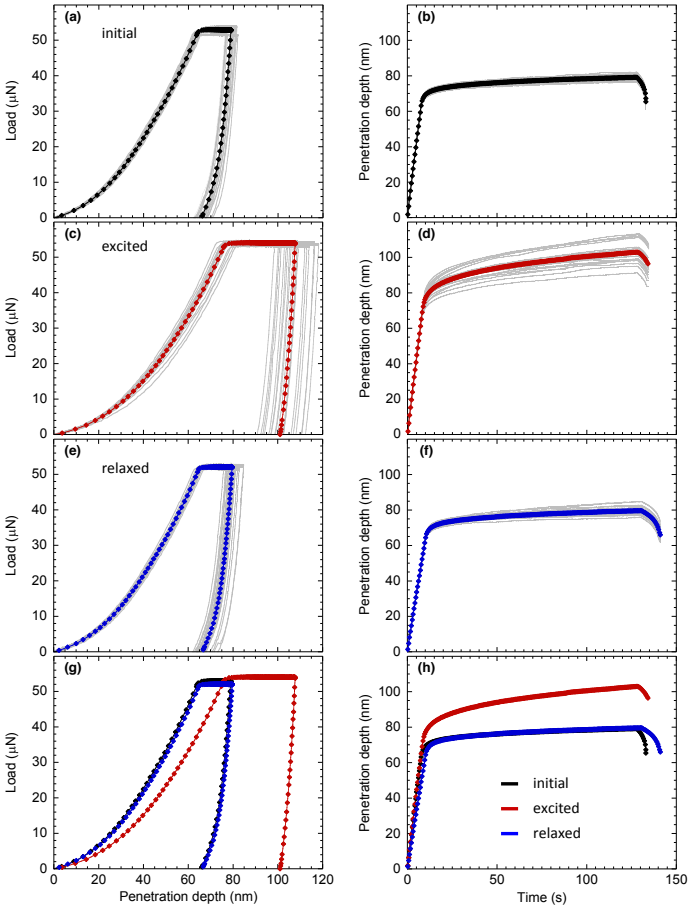

Fig. 6 $P-h$ curves and $h-t$ curves measured on PMMA-DR1 with $P_{max} = 50\ \mu$N , in the initial state before illumination (a,b), in the excited state during illumination (c,d) and in the relaxed state 30 minutes after illumination (e,f). The grey curves represent the multiple tests performed in each state. The average curves (g,h) are drawn with colored symbols.

area estimated following the Oliver and Pharr's method as shown in **Figure 1a** . Analogously, for the effective Poisson's ratio ν_c, we use the averaging formula:[47]

$$\nu_c = 1 - \left[\frac{(1-\nu_s)(1-\nu_f)}{1-(1-I_1)\nu_f - I_1\nu_s} \right] \tag{14}$$

for which the weighting function I_1 reads:

$$I_1 = \frac{2}{\pi}\arctan\left(\frac{d}{a}\right) + \frac{1}{\pi}\frac{d}{a}ln\left(\frac{1+(d/a)^2}{(d/a)^2}\right) \tag{15}$$

The value of ν_c is derived from Eq. 14, where $\nu_s = 0.22$ is assumed for Poisson's ratio of glass and $\nu_t = 0.37$ is assumed for the Poisson's ratio of the azobenzene containing film.[55] We assume these values to be invariant with respect to the illumination conditions since the film temperature does not significantly vary (and remains well below the glass transition temperature T_g) with the low laser power density that we use.[56] The value of G_c can be derived from the measured indentation modulus M as explained in Section II:

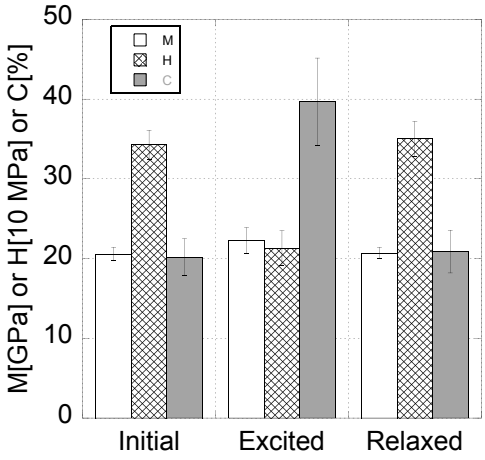

Fig. 7 Histograms of the indentation modulus (M), hardness (H) and creep (C) for the initial, excited and relaxed states (standard deviations are indicated by the error bars) for 250 nm thick azobenzene PMMA film. Actual values of H have to be multiplied tenfold.

$$G_c = \frac{E_c}{2(1+\nu_c)} = -\frac{1}{2(1+\nu_c)}\frac{(\nu_c^2-1)ME_i}{E_i - M + M\nu_i^2} \tag{16}$$

Table 2 summarizes the estimated values of the film elastic modulus E_f for the three states. It is interesting to notice that the effect of the substrate on the measured composite stiffness becomes more important under illumination since I_0 reduces from 41% in the dark, down to 34 % under optical excitation. The reason is that, while changing the mechanical properties of the azopolymer, light also affects the size of the film volume probed by nanoindentation. We conclude that the film modulus E_f slightly reduces under illumination (from 8.8 GPa to 8.5 GPa) in spite of the increase in M due to the higher proximity effect of the glass substrate. Furthermore, it is important to mention that our study is limited to a fixed loading/unloading rate of 10 μN s^{-1}, while the results may depend on the strain rate sensitivity of the azobenzene containing polymer, as shown by Vapaavuori et al.[33] Thus, the estimated values of E_f shall be taken as a first order approximation and further tests at different loading rates and advanced finite element analysis may be required to confirm these values.

Table 2 Values of the mechanical parameters of the 250 nm thick PMMA-DR1 film deposited on a glass substrate, deduced from the measurements presented in **Figure 5** and **Figure 6**.

	Initial	Excited	Relaxed
d/a	0.90	0.70	0.92
I_0	41%	34%	41%
I_1	70%	64%	70%
ν_s	0.22	0.22	0.22
ν_f	0.37	0.37	0.37
ν_c	0.33	0.32	0.33
G_s [GPa]	34.7	34.9	34.7
G_f [GPa]	3.2	3.1	3.3
G_c [GPa]	7.0	7.7	7.0
E_f [GPa]	8.8	8.5	9.0

Analogously to G_c, the measured hardness H_c results from two contributions, the one of the film H_f and the one of the substrate H_s. We assume that the composite hardness H_c follows the analytical law for a soft film on a hard substrate:[57]

$$H_c = H_s(1-I_H) + H_f I_H \tag{17}$$

where I_H, the weighting function, is given by:

$$I_H = exp\left(-\frac{Y_f}{Y_s}\frac{E_s}{E_f}\left(\frac{h_{max}}{d}\right)^2\right) \tag{18}$$

The quantities Y_f and Y_s are the material yield stresses of the film and substrate, respectively. Since Y_f may also change with illumination, a parametric variation of H_f as a function of the ratio Y_f/Y_s can be deduced from the measurement of H_c in the dark and under illumination (**Figure 8**).

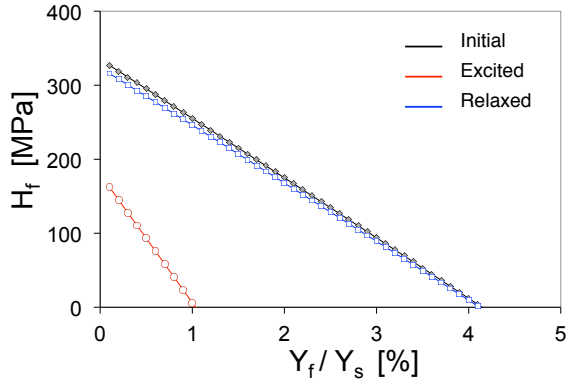

Fig. 8 Variation of the film hardness H_f as a function of the yield stress ratio Y_f/Y_s deduced from the measurements of H_c in the three film states (initial, excited and relaxed), according to Eq. 17.

Within the limit of validity of the Eq.17, which is $Y_f/Y_s < 5\%$, **Figure 8** shows a significant decrease in the $H_f(Y_f)$ curve under illumination which is at the origin of the diminution of the measured value of H_c. However, this analysis does not allow evaluating independently the changes in H_f and Y_f. Extracting information on the initial yield stress from nanoindentation experiments[58] is not trivial in our case since it would require to perform experiments with different loads on thicker samples, which would exhibit different photomechanical responses.

4.3 Light-induced change in the creep recovery

In the second experimental procedure (Experiment 2) the load is decreased from P_{max} to P_2 during the time τ_{U1} and the load P_2 is maintained during the time τ_{U2} (**Figure 4(b)**). The creep recovery curves $(h-t)$ are shown on **Figure 9** in the initial and excited states. The asymptotic behavior of the penetration depth, common to both states expresses the partial recovery of the viscous deformation. Indeed upon unloading, the penetration depth suddenly reduces due to the elastic deformation, followed by a slow creep regime. This could be related to the viscoelastic behaviour of an uncross-linked polymer, whose molecular chains are weakly attached to each other.[59] The illuminated material shows a creep recovery smaller than the one measured in the initial state. Moreover, the characteristic time of the creep recovery is much shorter than that of the creep under loading. Under illumination the material has developed a greater irreversible creep during the holding phase, which cannot be recovered after unloading. Therefore, since the permanent deformation, which is the irreversible penetration depth upon unloading, increases under illumination, we can conclude that illumination favours the viscoplastic behaviour of the material.

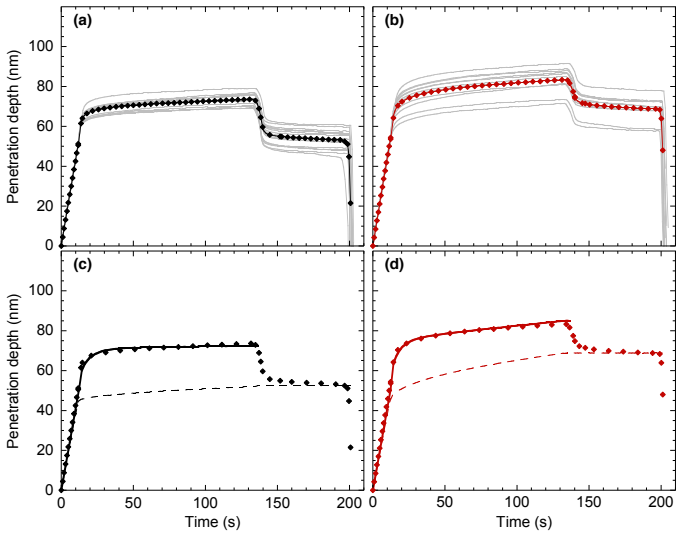

Fig. 9 $h-t$ curves measured in the initial state (a) and excited state (b) during the creep recovery test (Experiment 2). For each state, average curves are represented by continuous black and red curves, respectively. Symbols represent the simulation by the Burgers model described in the text. The irreversible plastic part deduced from the model is indicated in (c-d) by dotted-dashed line.

To determine the reversibility of the creep deformation, one needs to compare the residual penetration depth h_r reached after full unloading at the end of the Experiment 2 procedure with the plastic penetration depth h_p developed at the end of the loading phase. As discussed in Section II, the latter can be obtained by assuming that the elastic modulus is constant during loading and unloading, so that the elastic penetration depth h_e for a conical indenter can easily be deduced from Equation 8.[41] The creep recovery can be estimated by the parameter ω defined as:

$$\omega = \frac{h_{max}-h_r}{h_{max}-h_p} \tag{19}$$

When $h_r = h_p$, $\omega = 1$, which means that the elastic deformation developed during the holding phase is fully recovered after unloading. Table 3 shows the values of h_{max}, h_r, h_p and h_e deduced from of the mean $h-t$ curves for the three states with indication of the creep recovery parameter. The light excitation notably reduces the creep recovery from 60% to 39%, which corroborates the viscoplastic behavior of the polymer film under illumination, while it increases the dissipated energy from 70% to 91%.

To model the creep recovery, we apply the Burgers model of

Table 3 Measured values of the different penetration depths for the three illumination conditions.

Variable	Initial	Excited	After
$h(\tau_L)$ $[nm]$	62	68	68
$h_c(\tau_L)$ $[nm]$	23	24	25
$h_p(\tau_L)$ $[nm]$	39	44	43
$h_{max}(\tau_L+\tau_H)$ $[nm]$	74	85	81
$h_r(\tau_L+\tau_H+\tau_U)$ $[nm]$	53	69	n.a.
Creep recovery ω	60%	39%	n.a.
Dissipated energy γ	70%	91%	n.a.

Figure 2a which includes both the reversible creep part (i.e., the Kelvin-Voigt element with E_2, η_2) and the irreversible part (i.e., the Maxwell element with E_1, η_1). **Figure 9** shows the comparison between the measured and the simulated creep curves. The best fitting parameters of the Burgers model are listed in **Table 4**. In order to accurately reproduce the increase in the irreversible creep observed under light, the fitting value of the irreversible viscosity η_1 diminishes from 1595 to 149 GPa.s as light is turned on, whereas no significant variation of the reversible viscosity η_2 is obtained. This diminution of the film viscosity under illumination is however less important than the one previously reported using a significantly different experimental configuration.[27,30] Interestingly the effect of light is also to shorten the characteristic time of the irreversible viscosity t_1, which drops from 0.7 to 0.07 s. The effective modulus E_{eff} of the film is simply estimated from the two springs in series.

Table 4 Calculated parameters extracted from the Burgers viscous model using Equations (7), (9) and (10).

	Initial	Excited
$h_p(\tau_L)/h(\tau_L)$ $[\%]$	88	88
E_1 $[GPa]$	2271	2274
E_2 $[GPa]$	1.5	1.1
η_2 $[GPa.s]$	13.3	7.7
$t_2=\eta_2/E_2$ $[s]$	8.6	7.0
η_1 $[GPa.s]$	1595	149
$t_1=\eta_2/E_1$ $[s]$	0.70	0.07
$E_{eff}^{-1}=E_1^{-1}+E_2^{-1}$ $[GPa]$	1.5	1.1

4.4 Dynamics of the photo-induced change in the material mechanical properties

The last experimental procedure (Experiment 3) aims at measuring the transient change in the material mechanical properties due to light excitation. For this purpose, we measure the penetration depth of the indenter when the light is successively switched on and off, while the film is submitted to a constant load of 50.6 μN (**Figure 10**). Turning on the light 60 s after holding the load constant, the penetration depth shows a sudden rise hinting to a very rapid softening of the material within less than a few seconds. It is likely that this transitory feature between two creep regimes is directly related to the building up of a photostationary equilibrium between trans and cis isomers, which occurs within the same timescale.[60]

When light is turned off, an unexpected striking effect is observed. The penetration depth rapidly rises up before the creep rate retrieves its typical value in the dark. This surprising behaviour is not fully understood, but we can note that the dynamics of the transitory response is slightly slower than the one observed when light is turned on and could be related to the thermally-activated relaxation of the cis population towards the trans configuration. The corresponding change in the organisation of the PMMA-DR1 chains may be at the origin of the observed phenomenon. The respective contribution of the trans-cis and cis-trans isomerization to the dynamics of the mechanical response of azo-polymers is also discussed in literature in the case of the photoactuation of DR1-doped PMMA fibers.[61,62] Further investigations as a function of light intensity could probably provide some clues of the role of the photoisomerization rate and of the change in the relative trans and cis populations.

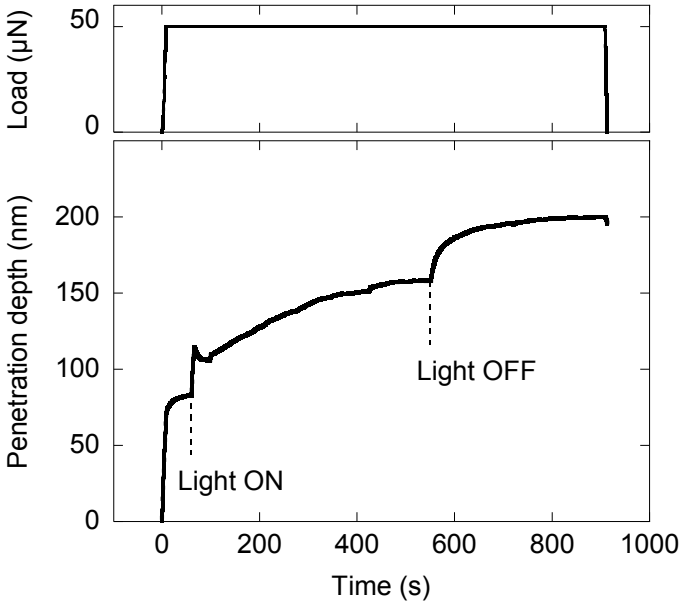

Fig. 10 Effect of on/off light switching during the creep experiment under constant load Pmax = 50.6 μN.

5 Conclusion

In the present work we have investigated the variation of the mechanical properties of DR1-containing PMMA thin films under light excitation by means of instrumented statistical nanoindentation measurements. With the state-of-the-art equipment used in this study, we have operated in a load range of a few tens of μN reaching corresponding penetration depths in the hundred of nm range, which is well-adapted to the study of thin polymer films. These experimental conditions are comparable with the conditions achieved with AFM-based nanoindentation, but with the advantage of independently control the load and the penetration depth. Moreover, quantitative measurements basically rely on the modeling of the nanoindenter tip, rather than on the several parameters needed to model the AFM cantilever deflection.

We performed three types of experiments: $P-h$ loading exper-

iments under illumination and in the dark, creep-recovery measurements and dynamical penetration measurements under light switching and constant load. Loading experiments show that optical excitation induces a significant decrease in the hardness H (-38%) and an increase in the creep C (+98%). A slight increase in the indentation modulus M (+8%) is observed which corresponds to a minute decrease in the Young's modulus of the PMMA-DR1 film E_f (-4%), when the contribution of the glass substrate is filtered out. The photo-induced modification of the material mechanical properties is mostly reversible: after light is turned off M, H and C retrieve their initial values. These results are in agreement with the general trend observed in similar materials up to now (**Table 5**).

The decrease of the irreversible viscosity η_1 by 1 order of magnitude (see tab.4) observed under illumination hints to fact that light strongly reinforces the viscoplastic behaviour of the film. This is confirmed by the 23% increase of the residual deformation h_r at the end of the creep test under illumination, and by the 30% increase in the dissipated energy γ_p. Additionally, the reduction of the hardness under illumination hints to the reduction of the plastic threshold (yield stress) of the viscoelastic behaviour.

Finally, we have measured the effect of light switching on the creep when a constant load is applied to the material. Turning on the light induces a stiff increase in the penetration depth. When light is turned off, while creep is expected to stop and even elastic recovery to occur, instead a stiff increase in the penetration depth is again observed. The two transitory features in the penetration depth triggered by the light switching can be related to the reorganization of the polymer chains caused by the building up of the photostationary equilibrium between the trans and cis azobenzene populations, when light is turned on, and the thermally activated relaxation of the cis-isomer population into the trans state, when light is turned off. The dynamics of the changes in the isomeric populations to reach a stationary state, when light is turned on and off, can be estimated by transient absorption measurements[60] and is found to indeed correspond to the observed transitory creep features. Further investigation of this phenomenon is in progress. Between these two transitory plastic deformation regimes, a slow, almost linear creep occurs that we likely relate to the photo-induced mass motion usually observed in azo-materials.

Table 5 Comparison of the light-induced changes in the mechanical properties of azobenzene-containing polymer films measured in the present work, with values previously reported for similar azo-polymer materials.

Ref.	Stiffness	Hardness	Creep recovery	Reversibility
[30]	-74%	n.a.	n.a.	n.a.
[33]	Reduced	Reduced	n.a.	n.a.
[34]	Reduced	Reduced	n.a.	n.a.
[35]	+50 to 150%	+100% to 300%	n.a.	Mostly irreversible
this work	-4%	-38%	60% dark 39% light	Completely reversible

6 Acknowledgments

This work was supported by the ANR (Contract No. COME-ON ANR-10-BLAN-1004). Dr. Sorelli was supported in part by the NSERC program.

References

1 Y. Zhao and T. Ikeda, *Smart Light-Responsive Materials: Azobenzene-Containing Polymers and Liquid Crystals*, John Wiley & Sons, 6th edn, 2009.

2 H. Rau, *Photochemistry and Photophysics Vol. 2*, CRC Press, Boca Raton, FL, 1990.

3 E. Rochon, P. Batalla and A. Nathanson, *Applied Physics Letters*, 1995, **66**, 136–138.

4 D. Y. Kim, S. K. Tripathy, L. Li and J. Kumar, *Applied Physics Letters*, 1995, **66**, 1166–1168.

5 T. Ikeda, M. Nakano, Y. Yu, O. Tsutsumi and A. Kanazawa, *Advanced Materials*, 2003, **15**, 201–205.

6 S. Angelos, E. Choi, F. Vogtle, L. De Cola and J. I. Zink, *The Journal of Physical Chemistry C*, 2007, **111**, 6589–6592.

7 N. K. Viswanathan, S. Balasubramanian, L. Li, S. K. Tripathy and J. Kumar, *Japanese Journal of Applied Physics*, 1999, **38**, 5928–5937.

8 F. Lagugne Labarthet, T. Buffeteau and C. Sourisseau, *The Journal of Physical Chemistry B*, 1999, **103**, 6690–6699.

9 N. Landraud, J. Peretti, F. Chaput, G. Lampel, J. P. Boilot, K. Lahlil and V. I. Safarov, *Applied Physics Letters*, 2001, **79**, 4562–4564.

10 T. Grosjean and D. Courjon, *Optics Express*, 2006, **14**, 2203–2210.

11 D. Garrot, Y. Lassailly, K. Lahlil, J. P. Boilot and J. Peretti, *Applied Physics Letters*, 2009, **94**, 033303.

12 F. Fabbri, Y. Lassailly, S. Monaco, K. Lahlil, J. P. Boilot and J. Peretti, *Phys. Rev. B*, 2012, **86**, 115440.

13 C. J. Barrett, A. L. Natansohn and P. L. Rochon, *The Journal of Physical Chemistry*, 1996, **100**, 8836–8842.

14 C. J. Barrett, P. L. Rochon and A. L. Natansohn, *The Journal of Chemical Physics*, 1998, **109**, 1505–1516.

15 J. Kumar, L. Li, X. L. Jiang, D.-Y. Kim, T. S. Lee and S. Tripathy, *Applied Physics Letters*, 1998, **72**, 2096–2098.

16 P. Lefin, C. Fiorini and J.-M. Nunzi, *Pure And Applied Optics*, 1998, **7**, 71–82.

17 T. G. Pedersen, P. M. Johansen, N. C. R. Holme, P. S. Ramanujam and S. Hvilsted, *Phys. Rev. Lett.*, 1998, **80**, 89–92.

18 S. P. Bian, J. M. Williams, D. Y. Kim, L. A. Li, S. Balasubramanian, J. Kumar and S. Tripathy, *Journal Of Applied Physics*, 1999, **86**, 4498–4508.

19 D. Bublitz, B. Fleck and L. Wenke, *Applied Physics B*, 2001, **72**, 931–936.

20 T. M. Geue, M. G. Saphiannikova, O. Henneberg, U. Pietsch, P. L. Rochon and A. L. Natansohn, *Phys. Rev. E*, 2002, **65**, 052801.

21 D. Barada, M. Itoh and T. Yatagai, *Journal Of Applied Physics*, 2004, **96**, 4204–4210.

22 K. Yang, S. Z. Yang and J. Kumar, *Physical Review B*, 2006, **73**, 165204.

23 M. L. Juan, J. Plain, R. Bachelot, P. Royer, S. K. Gray and G. P. Wiederrecht, *Applied Physics Letters*, 2008, **93**, 153304.

24 V. Toshchevikov, M. Saphiannikova and G. Heinrich, *The Journal of Physical Chemistry B*, 2009, **113**, 5032–5045.

25 T. Srikhirin, A. Laschitsch, D. Neher and D. Johannsmann, *Applied Physics Letters*, 2000, **77**, 963–965.

26 N. Mechau, M. Saphiannikova and D. Neher, *Macromolecules*, 2005, **38**, 3894–3902.

27 M. Nowicki, A. Richter, B. Wolf and H. Kaczmarek, *Polymer*, 2003, **44**, 6599 – 6606.

28 M. Moniruzzaman, P. Zioupos and G. Fernando, *Scripta Materialia*, 2006, **54**, 257 – 261.

29 H.-K. Kim, X.-S. Wang, Y. Fujita, A. Sudo, H. Nishida, M. Fujii and T. Endo, *Macromolecular Chemistry and Physics*, 2005, **206**, 2106–2111.

30 P. Karageorgiev, D. Neher, B. Schulz, B. Stiller, U. Pietsch, M. Giersig and L. Brehmer, *Nature Materials*, 2005, **4**, 699–703.

31 T. C. T. Ting, *J. Appl. Mech.*, 1966, **33**, 845–854.

32 L. H. Sperling, *Introduction to Physical Polymer Science, 2nd Ed.*, Wiley, NY, 1992.

33 J. Vapaavuori, Z. Mahimwalla, R. R. Chromik, M. Kaivola, A. Priimagi and C. J. Barrett, *J. Mater. Chem. C*, 2013, **1**, 2806–2810.

34 J. M. Harrison, D. Goldbaum, T. C. Corkery, C. J. Barrett and R. R. Chromik, *J. Mater. Chem. C*, 2015, **3**, 995–1003.

35 A. Richter, M. Nowicki and B. Wolf, *Molecular Crystals and Liquid Crystals*, 2008, **483**, 49–61.

36 N. Jennet, M. Goken and K. Durst, *Philosophical Magazine*, 2011, **91**, 1035–1036.

37 W. Oliver and G. Pharr, *Journal of Materials Research*, 1992, **7**, 1564–1583.

38 B. Blocken and J. Carmeliet, *Journal of Wind Engineering and Industrial Aerodynamics*, 2004, **92**, 1079 – 1130.

39 A. C. Fischer-Cripps, *Nanoindentation*, Springer-Verlag New York, 2011.

40 Z. Wu, T. A. Baker, T. C. Ovaert and G. L. Niebur, *Journal of Biomechanics*, 2011, **44**, 1066 – 1072.

41 I. N. Sneddon, *Mathematical Proceedings of the Cambridge Philosophical Society*, 1948, **44**, 492–507.

42 L. Chen, A. Ahadi, J. Zhou and J.-E. Stahl, *Procedia CIRP*, 2013, **8**, 334 – 339.

43 N. Conte, *CSM Application Bulletin*, 2007, **23**, 1–2.

44 F. Fabbri, D. Garrot, K. Lahlil, J. P. Boilot, Y. Lassailly and J. Peretti, *The Journal of Physical Chemistry B*, 2011, **115**, 1363–1367.

45 J. Nohava, N. Randall and N. Conte, *Journal of Materials Research*, 2009, **24**, 873–882.

46 C. Schuh and T. Nieh, *Journal of Materials Research*, 2004, **19**, 46–57.

47 O. Goodman and B. Derby, *Acta Materialia*, 2011, **59**, 1790 – 1799.

48 J. Howell, J. Hellmann and C. Muhlstein, *Materials Letters*, 2008, **62**, 2140 – 2142.

49 J. Gong, H. Miao and Z. Peng, *Acta Materialia*, 2004, **52**, 785 – 793.

50 T. Jin, X. Niu, G. Xiao, Z. Wang, Z. Zhou, G. Yuan and X. Shu, *Polymer Testing*, 2015, **41**, 1 – 6.

51 J. Hay and B. Crawford, *Journal of Materials Research*, 2011, **4**, 727–738.

52 A. Rar, H. Song and G. Pharr, Symposium Thin Films: Stresses and Mechanical Properties IX, 2001.

53 J. Antunes, J. Fernandes, N. Sakharova, M. Oliveira and L. Menezes, *International Journal of Solids and Structures*, 2007, **44**, 8313 – 8334.

54 H. J. Gao, C.-H. Chiu and J. Lee, *International Journal of Solids and Structures*, 1992, **29**, 2471–2492.

55 A. F. Yee and M. T. Takemori, *Journal of Polymer Science: Polymer Physics Edition*, 1982, **20**, 205–224.

56 N. Mechau, D. Neher, V. Boerger, H. Menzel and K. Urayama, *Applied Physics Letters*, 2002, **81**, 4715–4717.

57 A. Bhattacharya and W. Nix, *International Journal of Solids and Structures*, 1988, **24**, 1287 – 1298.

58 A. Clausner and F. Richter, *European Journal of Mechanics - A/Solids*, 2015, **51**, 11 – 20.

59 J. D. Ferry, *Viscoelastic Properties of Polymers, 3rd Edition*, J. Wiley and Sons, NY, 1980.

60 D. Garrot, *PhD thesis*, Universite Paris-Sud, 2006.

61 S. Bian, D. Robinson and M. G. Kuzyk, *J. Opt. Soc. Am. B*, 2006, **23**, 697–708.

62 X. Ye and M. G. Kuzyk, *Optics Communications*, 2014, **312**, 210 – 215.

Table of contents entry :

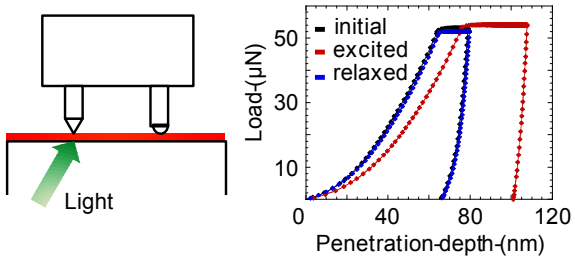

Statistical instrumented nanoindentation measurements demonstrate the large increase in the viscoplastic behavior of azo-polymer thin films under light excitation.